MEASUREMENTS OF MICROWAVE EMISSION FROM A FOAM COVERED, WIND DRIVEN SEA

W. NORDBERG
J. CONAWAY
DUNCAN B. ROSS
T. WILHEIT

Submitted for Publication to
Journal of Atmospheric Sciences
October 1970

OCTOBER 1970

GODDARD SPACE FLIGHT CENTER
GREENBELT, MARYLAND

X-650-70-384

Preprint

MEASUREMENTS OF MICROWAVE EMISSION FROM A FOAM COVERED, WIND DRIVEN SEA

W. Nordberg
J. Conaway
Duncan B. Ross*
T. Wilheit

October 1970

GODDARD SPACE FLIGHT CENTER

Greenbelt, Maryland

*Now with ESSA Air-Sea Interaction Laboratory, Miami, Fla.

ABSTRACT

Measurements were made from aircraft of the 1.55 cm microwave emission from the North Sea and North Atlantic at surface wind speeds ranging from less than 5 $msec^{-1}$ to 25 $msec^{-1}$. Brightness temperatures in the nadir direction increased almost linearly with wind speed from 7 msec to 25 $msec^{-1}$ at a rate of about 1.2 C per meter sec^{-1}. At 70° from nadir the rate was 1.8 C per meter sec^{-1}. This increase was directly proportional to the occurrence of white water on the sea surface. At wind speeds less than 7 $msec^{-1}$, essentially no white water was observed and brightness temperatures in the nadir direction were about 120 K; at wind speeds of 25 $msec^{-1}$ white water cover was on the order of 30 percent and average brightness temperatures at nadir were about 142 K. Maximum brightness temperatures for foam patches large enough to fill the entire radiometer beam, were 220 K.

1. Introduction

Considerable interest has been devoted to the quantitative measurement of sea surface roughness, on a global scale, from spacecraft and to the possible derivation of surface winds from these measurements (NAS Summer Study 1969). For this reason, we measured the microwave emission at 1.55 cm over the North Atlantic and the North Sea in March 1969 over a wide range of sea surface, wind, and cloud conditions in order to establish a quantitative relationship between the emission and the sea state and to delineate parameters such as surface winds, foam cover, wave height and cloud cover that would affect this relationship.

Earlier measurements (Nordberg, et. al., 1969) over the Salton Sea have shown that the microwave emission observed at all nadir angles from 0 to 50°, at a wavelength of 1.55 cm, is considerably greater from a rough water surface than from a smooth one. Stogryn (1967) had predicted that increases in microwave emission from rough water could be observed only at nadir angles greater than 30°. However, Stogryn's calculations were addressed primarily to the effect of the large scale wave geometry on the emission and did not, for example, account for foam and spray. We have, therefore, conducted these observations at high wind speeds and extensive foam cover to investigate further this discrepancy between theory and earlier observations.

2. Description of Experiment

Measurements were made from the NASA Convair 990 air-borne observatory. Primary instruments carried by the aircraft were:

(1) A radiometer measuring horizontally polarized radiation at 1.55 cm wavelength within a 2.8° x 2.8° field of view which was scanned perpendicularly to the aircraft's flight path over a nadir angle range of ±50 degrees. The same instrument was used in the Salton Sea observations; it was built by the Space Division of Aerojet General Corporation (Oister and Falco 1967).

(2) A Laser Geodolite of the Spectra-Physics Corporation to measure the ocean wave height spectrum.

(3) An infrared radiometer, similar to the Medium Resolution Infrared Radiometer (MRIR) flown on Nimbus satellites (Nimbus III User's Guide 1969), to determine the sea surface temperature from emission measurements at wavelengths between 10.6 and 11.6 μm.

(4) Standard, airborne navigation systems, both doppler and inertial, with which wind speed and direction at the aircraft altitude were measured.

(5) A Vinton 70 mm camera, pointing at nadir with a square field of view of about 68° to photograph sea surface and cloud conditions.

In addition, the aircraft carried standard instrumentation for altitude, attitude, speed, and ambient temperature measurements and auxiliary cameras. A non-scanning, nadir viewing 3 cm microwave radiometer with a field of view of about 13° x 13° was provided by the Jet Propulsion Laboratory for comparison with the 1.55 cm measurements.

The aircraft was based at Shannon, Ireland. Two flights, averaging 5 hours each, were made over the North Sea and four flights, equally long, covered a

region of the North Atlantic between Iceland and Ireland. In general, passes were made over each area of interest at several altitudes between 120 and 12,000 meters to differentiate the effects of atmospheric and surface emission.

Surface wind speeds ranged from calm to 25 $msec^{-1}$. They were obtained by extrapolation of the aircraft measured ambient wind speeds at the lowest flight altitudes under the assumption that wind speed decreased exponentially toward the surface (Ross et. al., 1970). This assumption was applied to all cases shown in Table 1, except Case E. In that case, examination of reduced geostrophic winds and ship reports lead us to assume that the wind speed increased from the height of the aircraft to the surface. We are very much indebted to Prof. Vincent Cardone of New York University for pointing this out to us.

Cloud conditions, observed visually and photographically from the aircraft, ranged from clear to strato-cumulus overcasts with moderate rain, over the numerous sea surface targets selected for the flights.

The 10-11 μm equivalent black body temperatures were taken to be equal to the sea surface temperature when measured with the infrared radiometer at the lowest altitudes. Temperatures ranged from 10 C at 50°N latitude over the Atlantic to 2 C over the coldest part of the North Sea.

Sea state varied from calm, with no white caps, to significant wave heights of about eight meters with over 30% coverage by foam with extensive streaking. Significant wave heights were determined by analysis of the wave spectra observed

with the laser Geodolite. Estimates of foam coverage were made by means of densitometry such that the total amount of white water contained in each frame of 70 mm photographs was determined. This method which was developed by one of us (D. Ross), attempts to account for the numerous and extensive white water streaks which were oriented with the wind direction. These streaks were observed at the higher wind speeds in addition to foam patches and white caps. The white water coverages obtained by this method are listed separately in Table 1 for white caps and streaks. Percentages for each case are averages resulting from several consecutive photographs. It was necessary to analyze several photographs for each case because of the variations in the foam cover obtained from individual frames.

Whenever possible, sea state, temperatures and winds measured with the aircraft were compared with the observations obtained from ocean vessels "I" and "J" (59°N, 19°W, and 53°N and 20°30'W respectively) and with analyses made by the Irish Meteorological Service at the Shannon Airport. There was never any significant discrepancy among these data. A complete log of all flights, including environmental and meteorological observations was compiled by Griffie, et. al., (1969). The specific conditions for which microwave measurements are reported here, are summarized in Table 1.

3. Results

Brightness temperatures measured at the 1.55 cm wavelength during six low altitude passes over the Atlantic and North Sea at wind speeds ranging from

less than 5 $msec^{-1}$ to about 25 $msec^{-1}$ were selected to illustrate their dependence on wind speed and foam cover (Figure 1). The recorded radiometer output was converted to radiances taking into account the calibrations performed on board the aircraft during each scan with two reference loads; one stabilized at 330 K and another terminated in a liquid nitrogen dewar. Antenna and radiometer characteristics, including effects of radiation received by the antenna through side lobes outside the 2.8° x 2.8° instantaneous field of view which were measured in the laboratory and against a known sky background prior to and after the expedition, were also taken into account in this conversion. The resulting radiances are expressed as brightness temperatures (°K) and are plotted in Figure 1 for the nadir viewing positions only. The radiometer field of view scanned from 50° left of nadir to 50° right of nadir, once every two seconds. Thus, the traces shown in Figure 1 consist of one data point per two seconds. They cover time segments corresponding to the sea, cloud and wind conditions listed in Table 1.

The plotted brightness temperatures (T_B) result from three radiation components received by the radiometer namely, radiation emitted to the aircraft by the sea surface, radiation emitted to the aircraft by clouds and atmospheric water vapor, and atmospheric radiation reflected toward the aircraft by the sea surface:

$$T_B = \epsilon T_W \tau_H + (1-\epsilon) T_S \tau_H + \int_O^H T_A(h) (\partial\tau/\partial h) dh, \qquad (1)$$

where:

T_W = Water Surface Temperature

T_S = Sky Brightness Temperature

T_A = Atmosphere Temperature

τ = Atmosphere Transmissivity

ϵ = Surface Emissivity

h = Height above Surface

H = Aircraft Altitude

The first, second, and third terms correspond to surface emission, reflected atmospheric radiation, and atmospheric emission respectively.

The cases listed in Table 1 were chosen such that atmospheric conditions, including cloud cover, were generally similar. In each of these cases, there was no measurable precipitation from the prevailing broken strato-cumulus clouds. Somewhat denser cloud cover encountered during higher wind speeds was almost compensated for by the lower atmospheric temperatures prevailing in these cases. For example, we have computed that the reflected radiation component for cases A and B of Table 1 (thin clouds but warm atmosphere) contributed about 9.5 C to the measured brightness temperature, while for cases E and F (thicker clouds, but cold atmosphere) this contribution was about 11 C. Thus, for the conditions listed in Table 1, the reflected component due to T_S can be assumed to be nearly constant, with variations certainly remaining smaller than 3 C. Also, the directly received emitted atmospheric radiation

was negligible when the aircraft was at low altitudes (150-200 m), since there were no clouds below the aircraft and the transmissivity was very near unity between the aircraft and the surface. In those cases, the integral term in Eq. (1) approaches zero.

Measurements of T_B were also made from high altitudes (> 5000 m) for the same conditions and generally within less than 30 minutes of the times listed in Table 1. Brightness temperatures were 6-8° C higher, depending on sea surface roughness, than corresponding brightness temperatures observed at the low altitudes. In each case, these increases relative to the low altitude passes, account quite precisely for the emitted atmospheric radiation term and for the decrease of τ_H from unity to about 0.95. The comparison between low and high altitude observations confirms our assertion that the measurements shown in Figure 1 were obtained under comparable atmospheric and cloud conditions.

At this wavelength, the measured brightness temperatures are essentially independent of the sea surface temperatures within the observed range, because ϵ varies inversely with the surface temperature such that ϵT_W in Eq. (1) is nearly constant.

Differences between the measured brightness temperatures for the various cases of Table 1 are then almost entirely due to differences in sea surface roughness. Brightness temperature differences between the lowest wind condition (case A) and each of the other cases were computed and plotted versus surface wind speeds in Figure 2. A systematic increase in emission with increasing

wind speed is clearly evident. The rate of increase is approximately 1.2 C per meter sec^{-1}. The Salton Sea measurements of 1968 (Nordbert et. al., 1969) are also shown and agree very well with this rate.

Measurements for the nadir direction only were plotted in Figures 1 and 2. At larger nadir angles, up to 70°, we have observed proportionally larger rates of increase. Figure 3 shows brightness temperatures as a function of nadir angle for a low and for the highest wind speeds listed in Table 1. Although the radiometer antenna scanned only to nadir angles of up to 50°, we were able to observe radiation from nadir angles up to 80° during banking of the aircraft. The two solid curves in Figure 3 were obtained by smoothing brightness temperature averages at each nadir angle for periods of 10-20 seconds during which the aircraft bank angle was held constant at 30°. The brightness temperature increase with wind speed increased from 1.2 C per $msec^{-1}$ at nadir to about 1.8 C per $msec^{-1}$ at 70° from nadir. This is qualitatively in accord with observations by Hollinger (1970), who reported an increase from 0.8° C per $msec^{-1}$ at 30° from nadir to 1.4° C per $msec^{-1}$ at 70° from nadir, for a much lower wind speed range.

The dashed curve in Figure 3 was computed for the atmospheric and sea surface temperature conditions observed for case B, but for a specular sea surface. The computed brightness temperatures at nadir are about 15 C higher than the observed ones. We believe that this discrepancy is partially due to errors in the absolute calibration of the radiometer and indicates that all brightness temperatures measured with this instrument should be increased by 10-15 C.

The relative calibration of the instrument was maintained at about ±1.5 C throughout all flights. Comparison of the slope of the dashed curve with the slope of curve B shows that the decrease of brightness temperatures with nadir angle is much steeper for the theoretical, specular and smooth water surface than for the real water surfaces, even at low wind speeds (Curve B). This suggests that the small scale roughness introduced even by very low winds causes a considerable brightness temperature increase at large nadir angles. The slopes of Curves B and F differ much less than those of curve B and the smooth water curve. This suggests that the rate of brightness temperature increase with nadir angle diminishes at the higher wind speeds. However, there remains a brightness temperature increase of at least 22 C with wind speed at all nadir angles, as shown by the off-set of curve F compared to curve B. This offset could be caused by the greater emission from white water such as foam and spray which would produce nearly the same brightness temperature increase at all nadir angles, depending only on the amount of foam cover.

Figure 2 shows that a nearly linear brightness temperature increase with wind speed occurs above a threshold of about 7 $msec^{-1}$. The measurements at 6 $msec^{-1}$ (case B) show no increase of T_B over the measurements at less than 5 $msec^{-1}$ (case A). Monahan (1969) has reported an abrupt increase in white cap coverage and spray density at 7 $msec^{-1}$ and Cardone (1969) has computed that the energy available for white cap production at wind speeds less than 7 $msec^{-1}$ is practically negligible. There is no evidence of any brightness temperature difference between cases A and B despite the fact that the sea surface was very

smooth for case A while extremely large swells (6 m) but no white caps were observed for case B. This suggests that the increase of microwave emission with wind speed, shown in Figure 2, is related mainly to the occurrence of white water (foam and spray). At lower wind speeds, where foam does not occur, the brightness temperature measured at all nadir direction is independent of wind speed. Foam has been suspected previously as a cause for increased microwave emission (Williams, 1969 and Droppleman, 1969).

Further evidence of the dependence of the microwave emission on foam cover can be found in the rapid brightness temperature fluctuations with time, shown in Figures 1c through 1e. In Figure 1d, for example, the average brightness temperature is about 132 K, but, instantaneous spikes frequently reach 140 K and two spikes exceed 155 K. Figure 1e, which corresponds to winds of 25 $msec^{-1}$, shows many more of these spikes. In this case, the average brightness temperature is about 142 K, but instantaneous spikes exceeding 150 K occur about every 30 seconds. Several of these spikes range between 175 and 190 K. From the photographs there is a strong implication that these spikes are caused by foam patches on the sea surface.

We have analyzed the instantaneous brightness temperatures measured at all scan angles over a period of 20 minutes, approximately centered on the time corresponding to Figure 1e, to determine the amplitude and frequency of brightness temperature spikes. We found that the maximum amplitude was about 220 K for seven spikes which occurred during that period. One such spike was clearly

coincident with the immense foam patch photographed in Figure 4d. The radiometer scanned the scenes shown in Figure 4 from left to right, with the aircraft having flown from bottom to top. Since the position of the scans on the photographs are not known exactly, and since at low altitudes scans were not contiguous, the foam patches may not always have filled the antenna field of view entirely. We assume that this occurred only when the maximum brightness temperatures of 220 K were measured.

The photographs of Figure 4 were taken over sea states corresponding to the brightness temperature measurements in Figures 1b through 1e, respectively. Aircraft altitudes ranged from 120 m to 450 m. Figure 4d was observed from 120 m and extends over about 200 m from top to bottom. The foam estimates (Table 1) were made from time series of photographs for each of the cases shown in Figures 4a through 4d. The increasing amounts of both foam patches and streaking with wind speed are quite apparent. We assume that such streaking and foam patches which were small relative to the radiometer field of view, raised the measured brightness temperatures uniformly throughout each scan, but that the largest patches of foam produced the temperature spikes which were more than 70 C above the average. It is, therefore, very important that estimates of foam coverage, as they relate to the microwave emission, include the effect of both foam patches and streaking. This has been attempted with the estimates of total foam cover listed in Table 1.

The brightness temperature spikes seen in Figures 1d and 1e were not observed when the aircraft was at higher altitudes, where each foam patch covered an area much smaller than that resolved by the instantaneous field of view of the radiometer. Figure 1f shows brightness temperatures measured from 5,500 m in the vicinity where the photograph of Figure 4d and the measurements shown in Figure 1e were made. No large spikes are evident in this case. At the aircraft height of 120 m (Figure 1e) each scan spot covered an area with a diameter of about 7 meters, while at the aircraft height of 5,500 m (Figure 1f) the diameter of the area covered was about 275 m. In the latter case, brightness temperatures show a much smoother pattern with no significant spikes because the characteristic diameter and spacing of the largest foam patches was indeed less than about 100 m (Figure 4d) and individual patches were not resolved by the radiometer.

Brightness temperature differences were plotted versus foam coverage in Figure 5, as determined from the photographs (solid line). There is a similar increase of brightness temperature with foam cover, as there is with wind speed. However, the rate of increase obtained from the small scale, single foam patch measurements, each representing 100% foam cover, (dashed line) is considerably greater than the rate determined from the large scale observations derived from the photographs for less than 40% foam cover (solid line). There are two possible explanations for this discrepancy:

(1) The estimates of streaking which account for a large portion of the white water coverage as determined from the photographs (Table 1) are subjective,

though internally consistent. Thus, foam cover as determined from the photographs may have been overestimated. This is also suggested by the fact that if foam cover is taken from Cardone's (1969) model, brightness temperature increases are consistent with the rate obtained for 100% foam cover (dashed line) which is independent of the estimates made from the photographs.

(2) Another possibility is that the total white water estimates made from the photographs are correct but that the effect of the streaks on the microwave emission is smaller than the effect of the white caps which produce the 100% foam cover spikes. In this case, the agreement with Cardone's model would be purely coincidental. Further microwave measurements under controlled conditions of foam and streaking should resolve this point.

It is noteworthy that the Salton Sea measurements made on 5 June 1968 are totally consistent with the North Sea and Atlantic measurements with regard to brightness temperature dependence on both wind speed and on foam cover.

Preliminary results from the 3 cm radiometer, flown simultaneously with the other instruments, indicate that the brightness temperature increase at this wavelength is about 8 C for a wind speed increase from calm to 13 $msec^{-1}$. Beyond 13 $msec^{-1}$ there is only a negligible increase in brightness temperature. However, because of instabilities in the radiometer, the measurements at the 3 cm wavelength cannot be considered as firm as those at 1.55 cm. We are indebted to Messrs. F. Barath and J. Blinn of the Jet Propulsion Laboratory and A. Edgerton of Aerojet General Corporation for making this, as yet unpublished, information available to us.

4. Conclusions

There is a definite increase in the thermal emission at 1.55 cm from the sea surface with increasing wind speed. On the average, this increase amounts to about 22 C in the nadir direction and 32 C at 70° from nadir for a wind speed increase from 7 to 25 $msec^{-1}$. For very low wind speeds, up to about 7 $msec^{-1}$, when foam cover is negligible, there is no increase in brightness temperatures. Compared to calm sea states, brightness temperatures are about 100 C higher when foam patches covering the radiometer field of view are observed. Thus, we conclude that the increased emission at 1.55 cm from a wind driven sea surface is primarily due to white water cover, while the effect of the wave slope geometry is negligible. The microwave emission at 1.55 cm from the sea surface is therefore a sensitive indicator of white water coverage and of wind speed at all nadir angles, at least to 50°.

We believe that an important parameter involved in the interaction between air and the sea surface, namely, the energy expended in the production of white water can be inferred from microwave brightness temperature measurements provided that:

(1) The consistent relationship between white water occurrence and wind speed reported here is confirmed and

(2) Microwave measurements are made at various wavelengths, both polarizations, and over a large range of nadir angles to separate the various effects of foam cover, cloud cover, and atmosphere and sea surface temperatures on the microwave emission.

Results from the observations reported here might provide a basis to test further developments or revisions of analytical models relating microwave emission to sea surface roughness.

5. Acknowledgements

There were several dozen individuals without whom these observations would not have been possible. We are unable to name all of them, but we acknowledge their dedicated contributions gratefully. We are expecially indebted to the NASA pilots and flight crew of the CV 990 observatory for carrying out the demanding flight operations that were required for these observations; to Mr. Earl Peterson of the NASA Ames Research Center for organizing the expedition and the Irish Meteorological Service for providing excellent weather forecasts and analyses to support our flight operations.

Table 1

CASE	A	B	C	D	E	F
DATE - March 69	19	13	13	10	19	14
TIME (GMT)	1321	1247	1117	1430	1023	1453
LOCATION	Atlantic Off Shannon	Atlantic Ship J	Atlantic Ship I	Atlantic Ship I	North Sea 57°N 3°E	North Sea 59°N 1°30'E
WIND SPEED (msec)	<5	6	13	16	17	25
SIGNIFICANT WAVE HEIGHT (m)	<1	6.0†	3.9	5.0	4.0	7.8
FOAM COVER (%)						
WHITE CAPS	—	—	3	7	5	5
STREAKS	—	—	11	15	19	32
TOTAL	—	—	14	22	30	37
TEMPERATURE (°C)						
SEA-SURF.	9	10	9	9	2	4
AIR-SURF.	10 (est.)	11	7	5	2	2
CLOUD BASE (m)	2,000	clear	300	800	600	150
TOP (m)	2,300	clear	2,100	2,000	2,000	5,000
BRIGHTNESS TEMP. (°K)						
HIGH ALTITUDE*	128**	—	—	138	138	148
LOW ALTITUDE	120	118	127	132	132	142

*Measured within 30 minutes of time shown
**Over Irish Sea at 1212 GMT
†All swell, no wind waves

References

Cardone, V. J., 1969, Specification of the wind field distribution in the marine boundary layer for wave forecasting. Geophysical Science Laboratory, New York University, Report No. TR69-1.

Droppleman, J. D., 1970, Apparent microwave emissivity of sea foam. J. Geophys. Res., 75(3), p. 696.

Griffee, L., J. Ledgerwood, D. Hill, W. E. Marlatt, 1969, Support data for NASA Convair 990 meteorological flight IV. Dept. of Atmospheric Science, Colorado State University, Ft. Collins, Colorado, p. 83.

Hollinger, J. P., 1970, Passive microwave measurements of the sea surface, J. Geophys. Res., (in press).

Monahan, E. C., Freshwater white caps. J. Atmos. Sci., Vol. 26, No. 5, p. 1026.

NAS Summer Study, 1967. Useful applications of earth-oriented satellites. Summer study on space applications, National Academy of Sciences, Washington, D. C.

Nimbus III User's Guide, 1969. Staff Members, Nimbus Project, National Aeronautics and Space Administration, Goddard Space Flight Center, Greenbelt, Maryland.

Nordberg, W., J. Conaway and P. Thaddeus, 1969, Microwave observations of sea state from aircraft. Q. J. of Royal Met. Soc., Vol. 95, No. 404, p. 408.

Oister, G., C. V. Falco, 1967, Microwave radiometer design and development. Fin. Rep. Contract No. NAS5-9680, Aerojet-General Corp., Space Division, 9200 East Flair Drive, El Monte, California.

Ross, D. R., V. Cardone and J. Conaway, 1970. Laser and microwave observations of sea surface conditions for fetch limited 35 to 50 knot winds. IEEE Transactions on Geoscience and Electronics, Vol. GE-8, No. 4, Oct. 1970, (in press).

Stogryn, A., 1967, The apparent temperature of the sea at microwave frequencies. IEEE Transactions on antennas and propagation, AP-15, No. 2, p. 278.

Williams, G. F., Jr., 1969. Microwave radiometry of the ocean and the possibility of marine wind velocity determination from satellite observations. J. Geophys. Res., 74(18), p. 4591.

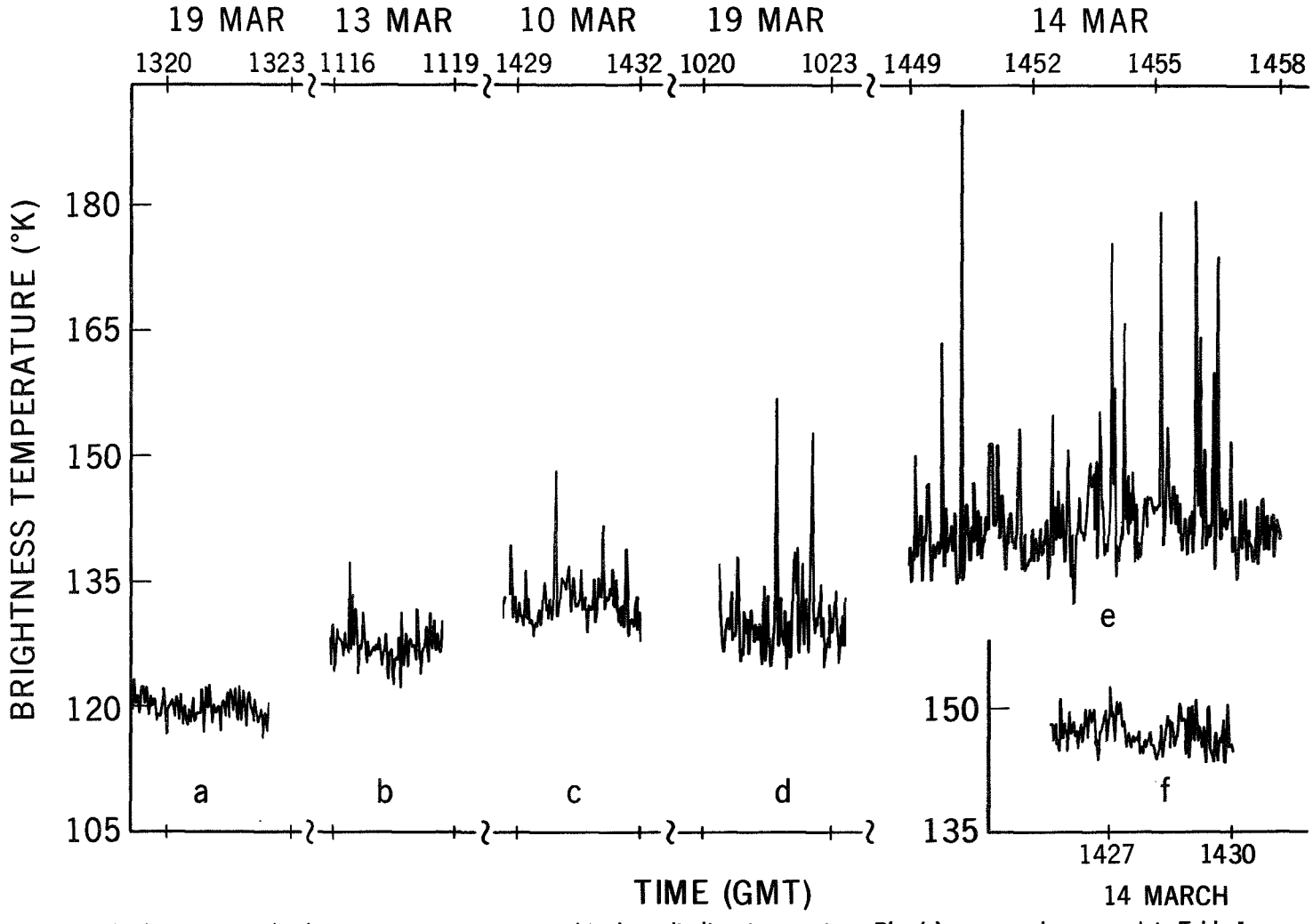

Figure 1. Instantaneous brightness temperatures measured in the nadir direction vs. time. Plot (a) corresponds to case A in Table 1. Plots (b) through (e) correspond to cases C through F in Table 1. All brightness temperatures in plots (a) through (e) were observed from heights of about 150 m. Brightness temperatures in plot (f) were observed from a height of about 5,500 m over approximately the same location as plot (e).

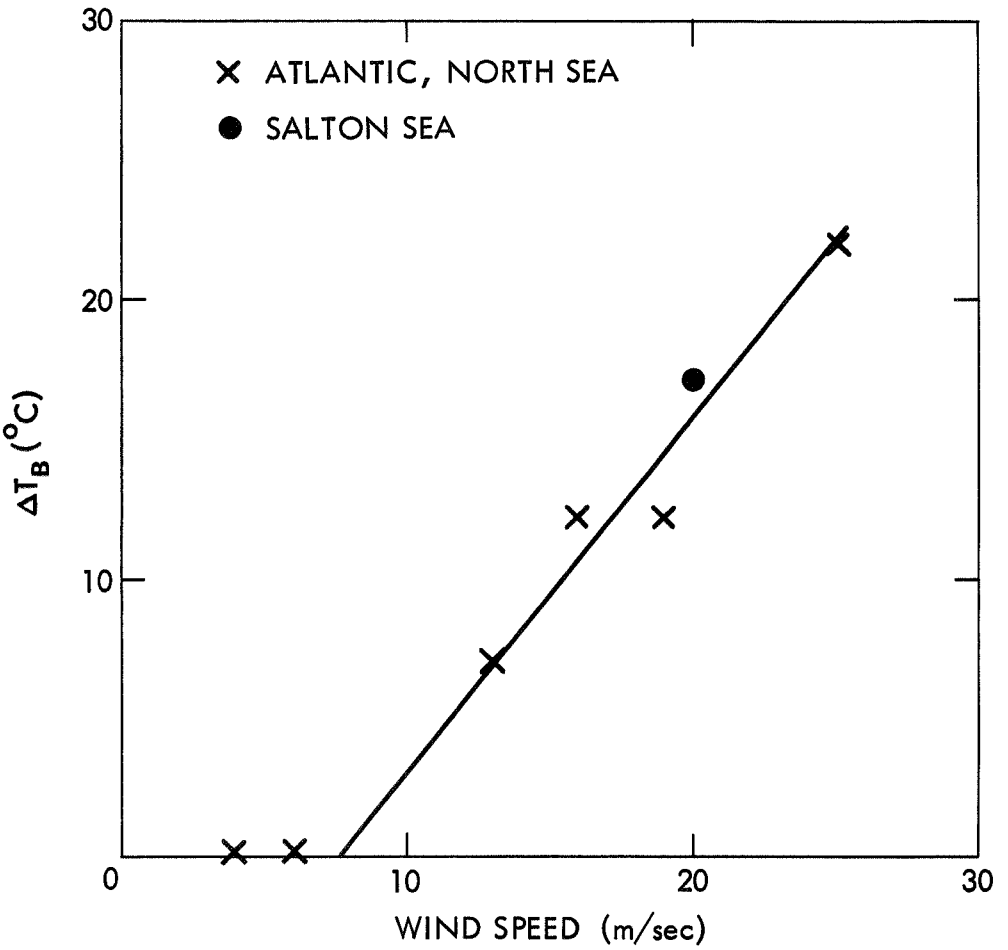

Figure 2. Brightness temperature differences between those measured at wind speeds less than 5 $msec^{-1}$ and higher wind speeds, vs. wind speed.

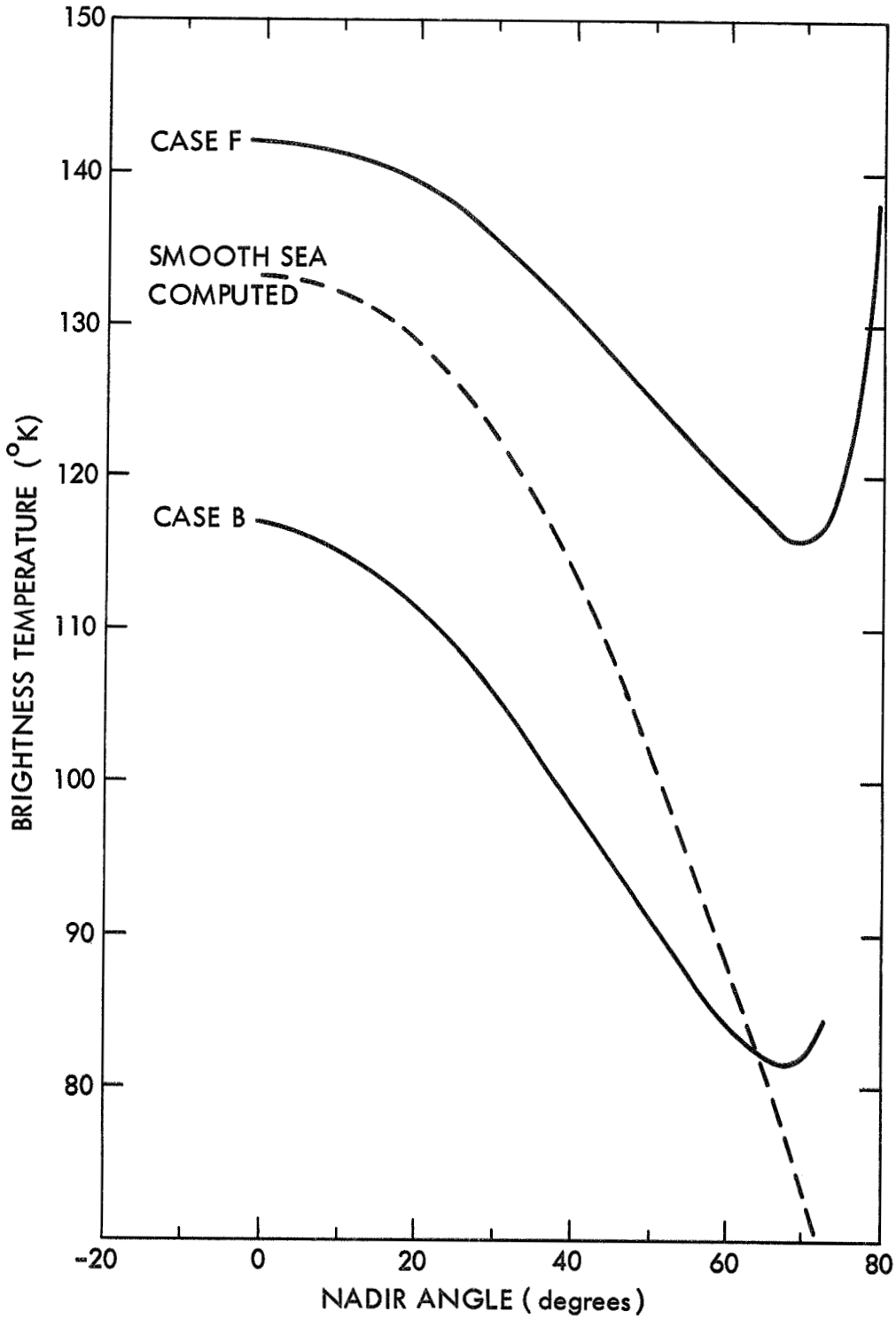

Figure 3. Brightness temperatures averaged for 10-29 second time periods for each antenna scan angle during 30° aircraft banks vs. nadir angle for case B of Table 1 (lower curve) and case F of Table 1 (upper curve). The dashed curve results from computed brightness temperatures for atmospheric and sea surface temperatures encountered in case B but for a smooth, specular sea surface.

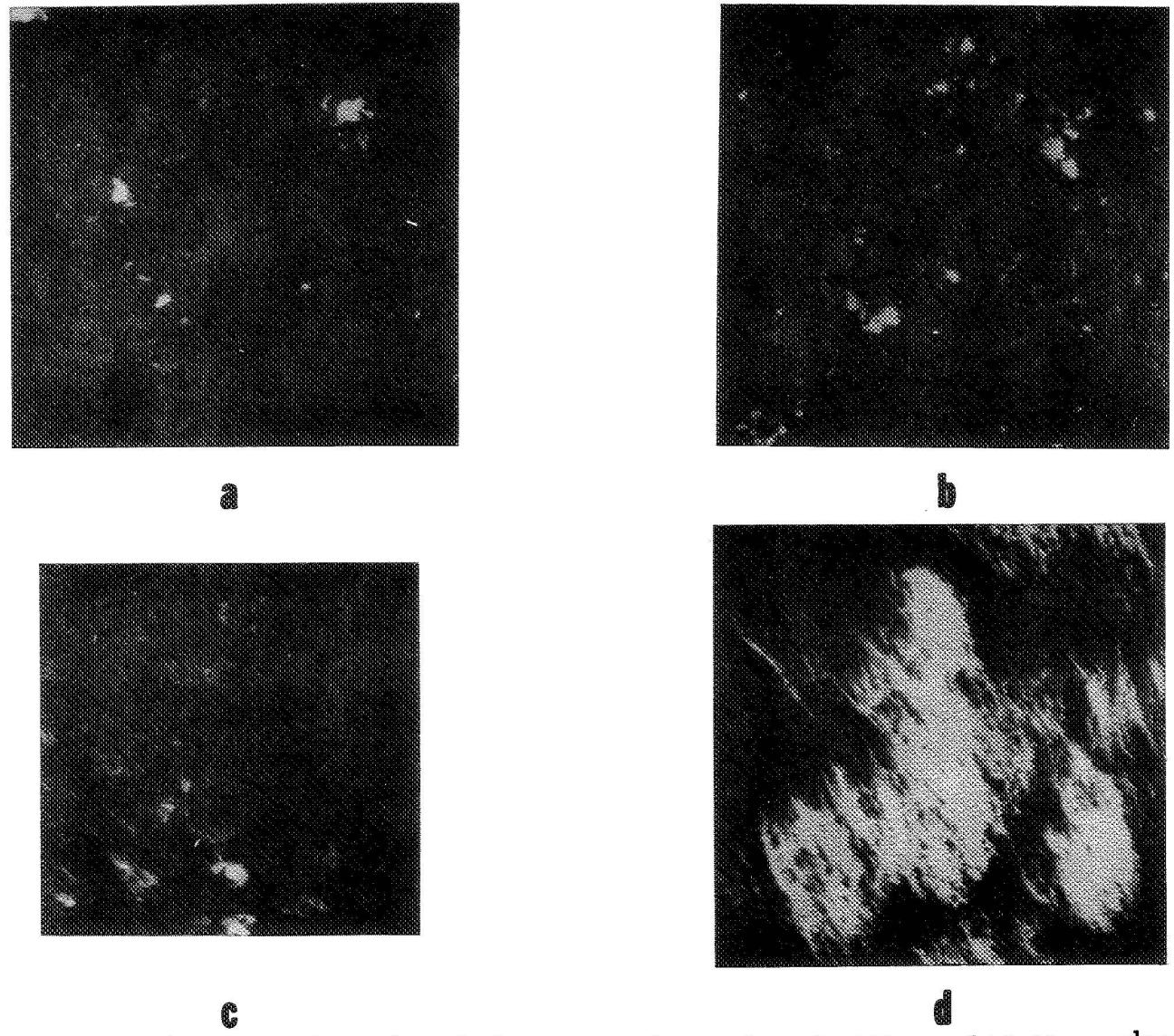

Figure 4. 70 mm photographs taken in the nadir direction at surface wind speeds of 13 $msec^{-1}$ (a), 16 $msec^{-1}$ (b), 18 $msec^{-1}$ (c) and 25 $msec^{-1}$ (d), corresponding to cases C through F respectively in Table 1.

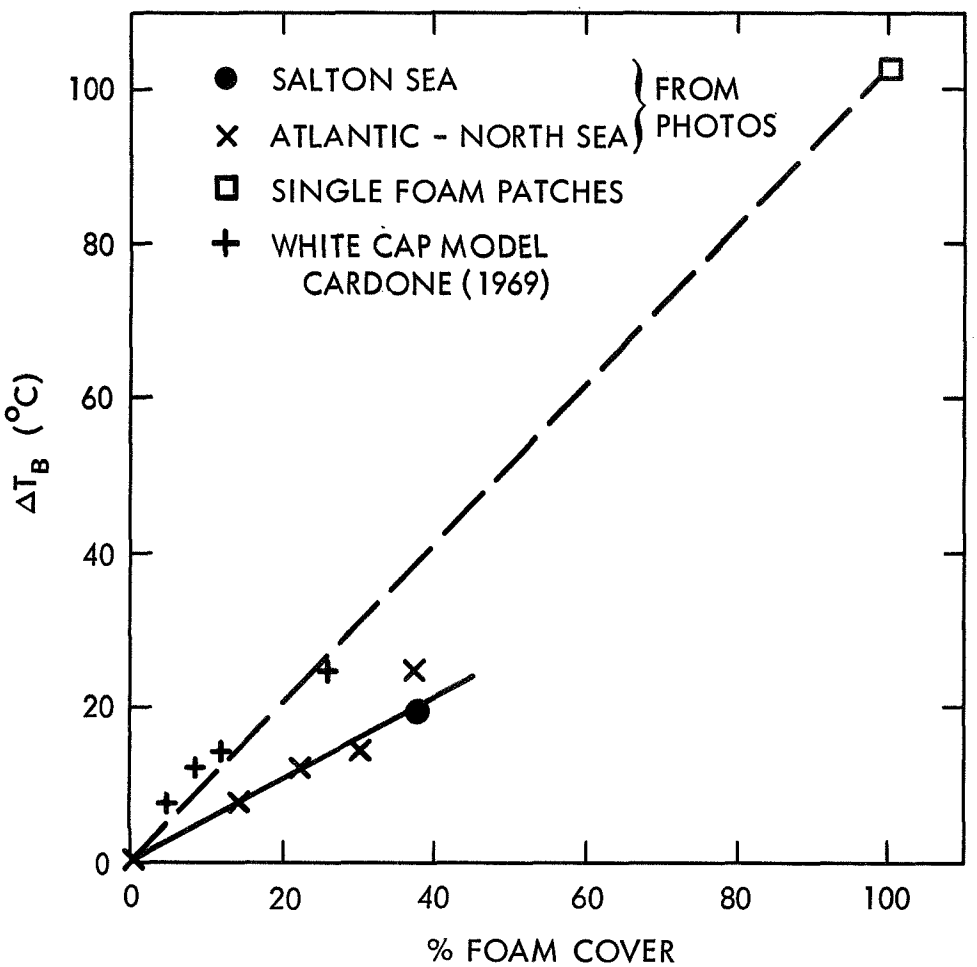

Figure 5. Brightness temperature differences between those measured at wind speeds less than 5 msec^{-1} and at higher wind speeds, vs. foam cover estimated from photographs, analytical model of Cardone and single foam patches covering the entire microwave radiometer beam as indicated by symbols in the graph.

Figure Captions

Figure 1 Instantaneous brightness temperatures measured in the nadir direction vs. time. Plot (a) corresponds to case A in Table 1. Plots (b) through (e) correspond to cases C through F in Table 1. All brightness temperatures in plots (a) through (e) were observed from heights of about 150 m. Brightness temperatures in plot (f) were observed from a height of about 5,500 m over approximately the same location as plot (e).

Figure 2 Brightness temperature differences between those measured at wind speeds less than 5 $msec^{-1}$ and higher wind speeds, vs. wind speed.

Figure 3 Brightness temperatures averaged for 10-20 second time periods for each antenna scan angle during 30° aircraft banks vs. nadir angle for case B of Table 1 (lower curve) and case F of Table 1 (upper curve). The dashed curve results from computed brightness temperatures for atmospheric and sea surface temperatures encountered in case B but for a smooth, specular sea surface.

Figure 4 70 mm photographs taken in the nadir direction at surface wind speeds of 13 $msec^{-1}$ (a), 16 $msec^{-1}$ (b), 18 $msec^{-1}$ (c) and 25 $msec^{-1}$ (d), corresponding to cases C through F respectively in Table 1.

Figure Captions (Continued)

Figure 5 Brightness temperature differences between those measured at wind speeds less than 5 $msec^{-1}$ and at higher wind speeds, vs. foam cover estimated from photographs, analytical model of Cardone and single foam patches covering the entire microwave radiometer beam as indicated by symbols in the graph.